

A DETAILED INVESTIGATION OF PHYSICAL AND BIOLOGICAL CLOGGING DURING ARTIFICIAL RECHARGE

S. VIGNESWARAN and RONILLO B. SUAZO

Environmental Engineering Division, Asian Institute of Technology, P.O. Box 2754, Bangkok, Thailand

(Received August 1, 1985; revised April 7, 1987)

Abstract. An attempt was made to study the physical and biological clogging during artificial recharge with an experimental model that simulates the artificial recharging practice by considering factors such as effective infiltration rate, media size and depth, and inundation period. Recharging was investigated experimentally in terms of suspended solids (SS) removal, 3-day biological oxygen demand (BOD₃) removal and chemical oxygen demand (COD) removal at different sand sizes and infiltration rates. To understand the physical phenomenon involved, the effect of suspended solids concentration and initial infiltration rate on cumulative discharge was studied and verified using a simple mathematical model. The simulated cumulative discharge profiles were comparable with the experimental profiles. This indicates that an empirical relationship can be successfully used to predict the biological clogging at different recharge rates. The effect on headloss was also discussed.

1. Introduction

In many countries of the world, groundwater is the main source of water supply. Groundwater supply, however, is limited and due to the excessive withdrawal from the underground aquifers, problems like salinity intrusion and land subsidence result. With the present urbanization and industrialization boom, wastewater disposal in these countries becomes a serious problem. Large and increasing volumes of effluent from treatment plants do not only necessitate efficient treatment systems but require disposal facilities as well. Therefore, the artificial recharge practice will not only be a means of disposal and restoration of the safe yield of underground aquifers but will also help to meet the ever increasing water demand.

Artificial recharge is the practice of releasing water over the ground surface with the use of simple structures like basins, wells, channels and ditches for the purpose of renovation, water conservation and the provision of the necessary pressure required to reverse the hydraulic gradient and to prevent problems associated with overdrafts (Todd, 1959). It can be achieved through water spreading or a recharge well. Water spreading methods release water over the ground surface and allow it to percolate into the ground thereby increasing the volume of water stored within the aquifer. The recharge well method is similar to a pumped well except that water is poured into the aquifer instead of being withdrawn by the pump. Artificial recharge physics or hydrology which describes the above methods is well known and can be found in a number of texts (Todd, 1959; Huisman and Olsthoorn, 1983).

The practice of artificial recharge is worldwide: notably in the United States, Europe, Australia, and Israel. In California, due to excessive withdrawal of groundwater, some 276 artificial recharge systems operate (Todd, 1959). Further, Todd estimated that as

of 1970 more than 400 cities in the United States were using treated effluent for agricultural irrigation or for groundwater recharge. Basin infiltration rates of 0.03 to 61 m day⁻¹ have been reported (Fetter and Holzmacher, 1974). Man-made infiltration pits, 100 m long and 3 m wide have been employed in Australia's artificial groundwater recharge project at Burdekin Delta (Besty, 1980). In this project, water is fed and allowed to percolate for about 4 weeks. Infiltration rates of up to 6 m day⁻¹ have been observed. In Israel, 90% of the known potential amount of water available is used annually and replenishment of groundwater is necessary (Harpaz, 1970). Seventy-nine percent of the recharging operations is by recharge well method and over 100×10^6 m³ of water is recharged every year. The system which is used to reclaim domestic wastewater consists of a series of anaerobic, facultative and aerobic lagoons, from which earth channels convey the effluent to the spreading basins where it is allowed to percolate (Amramy, 1965). In Sweden, river water is recharged at the rates of 0.9 to 4.6 m day⁻¹ (Winqvist and Marelius, 1970), and at 0.15 to 0.46 m day⁻¹ in Holland (Vecchioli and Ku, 1971). In Germany, river water is recharged at a design rate of 2.4 m day⁻¹. In Britain, a variety of industrial wastes have been injected into underground wells and boreholes (Todd, 1959).

Although artificial recharge is practiced throughout the world, no detailed study has been conducted to investigate the effects of the clogging mechanism involved within the sand pores. Such study would be helpful in the design of the artificial recharge facility and in determining the suitability of artificial recharge in particular cases.

2. Past Studies

The mechanisms in soil clogging are physical, biological, and chemical. Physical clogging is similar to flow through porous media, or specifically to particle deposition in deep bed filtration. Literature is available on this aspect of deep bed filtration. Obviously, the major factors affecting the particle deposition are suspended solids concentration of the recharging water, soil size and distribution, and porosity. Thus, it can be investigated by headloss developments and by specific accumulation. A detailed study was carried out to estimate the clogging of sand by inert particles using conventional filtration mathematical models (Vigneswaran *et al.*, 1985; Thiagaram, 1982; Vigneswaran and Thiyagaram, 1984). On the other hand, in a particular experiment, Okubo and Matsumoto (1979, 1983) observed a decrease in headloss at 1 cm depth after a constant headloss value, which may have resulted from biological decomposition within the clogging surface layer.

The effect of soil media size in recharge water renovation during artificial recharge had been reported by De Vries (1972). As expected, the smaller the size of the soil media, the better is the BOD₅ removal.

Biological clogging is believed to follow physical clogging, though both phenomenon co-exist at the later stage of recharge. It can be thought of as a result of two factors: biological growth and the accumulation of by-products resulting from the decomposition of biological growth. The first factor, the biological growth, reduces the size of soil pores.

In the second factor, the by-products resulting from biological degradation accumulate and consequently reduce the size of the interstices, causing reduction in the volume of discharge which eventually result in permanent clogging.

With the accumulation of suspended matter in the recharging medium, biological growth develops, which in turn seals the pores and reduces the infiltration rate. The factors affecting biological clogging are algae and bacterial growth, sedimentation of fine organic particles and interaction of bacteria, algae, and sediments and even the accumulation of undissolved gas and other products of microbial decomposition which seal the soil pores. Allison (1947) showed the effect of bacterial growth on the behavior of the infiltration rate. Wood and Basset (1975) observed that the loss infiltration rate was associated with anaerobic microbial growth. A study of microbial growth in surface spreading methods showed that the clogging due to biological matter predominates at the top few centimeters (Ripley and Saleem, 1973). Even in the case of injection wells, the rise in injection head had been found to reach its maximum when large amounts of biodegradable matter are present in the injection water (Huisman and Olsthoorn, 1983). Sludge layer formation in the soil surface has been reported to cause loss in infiltration rate (De Vries, 1972). In investigating the effect of bacterial growth on the infiltration rate directly, Avnimelech and Nevo (1964), Mitchell and Nevo (1964), and Nevo and Mitchell (1967) measured the concentrations of polysaccharides and polyuronides which are components of bacteria cell capsules. They found a correlation between the increase in their concentrations and the loss in hydraulic conductivity. Gas production associated with nitrification was even reported to decrease the infiltration rate (Lance and Whistler, 1973).

A more detailed study about biological clogging during artificial recharge was conducted by Okubo and Matsumoto (1979, 1983) using synthetic wastewater. Factors found to affect biological clogging were initial specific discharge, influent soluble organic carbon concentration, temperature and influent organic suspended solids concentration. They introduced a mathematical model in order to quantify the effect of the factors involved on the cumulative discharge. The proposed model is introduced in a later section.

Chemical clogging may occur at the aquifer due to the complex chemical reactions which result from the mixing of water of different compositions. The various types of blocking may be caused by the following: precipitated metabolic products of autotrophic bacteria including iron hydroxide, ferrous bicarbonate, and calcium carbonate, chemical interaction of the dissolved chemicals in the recharge water, reactions of recharged water and native groundwater of different chemical characteristics and reaction of high Na content waters with soil particles causing deflocculation of the soil. However, it is very complex to include the three soil clogging mechanisms in one model. This study is confined to the investigation of physical and biological clogging of sand by the application of effluent from a domestic sewage oxidation pond. The objective of this study is to investigate the effect of sand size, depth and initial infiltration rate in terms of BOD₃, COD, and SS removal during artificial recharge using effluent from a domestic sewage oxidation pond.

3. Experimental Set-Up and Experimental Analysis

Four laboratory-scale experiments were carried out and the schematic diagram of the experimental set-up is shown in Figure 1. The filter columns used were 10 cm in diameter and 100 cm long. Sampling taps were located at 1.5, 4.5, 12.5, and 22.5 cm from the sand surface of each unit. The headloss was also measured at different depths using piezometric tube arrangement.

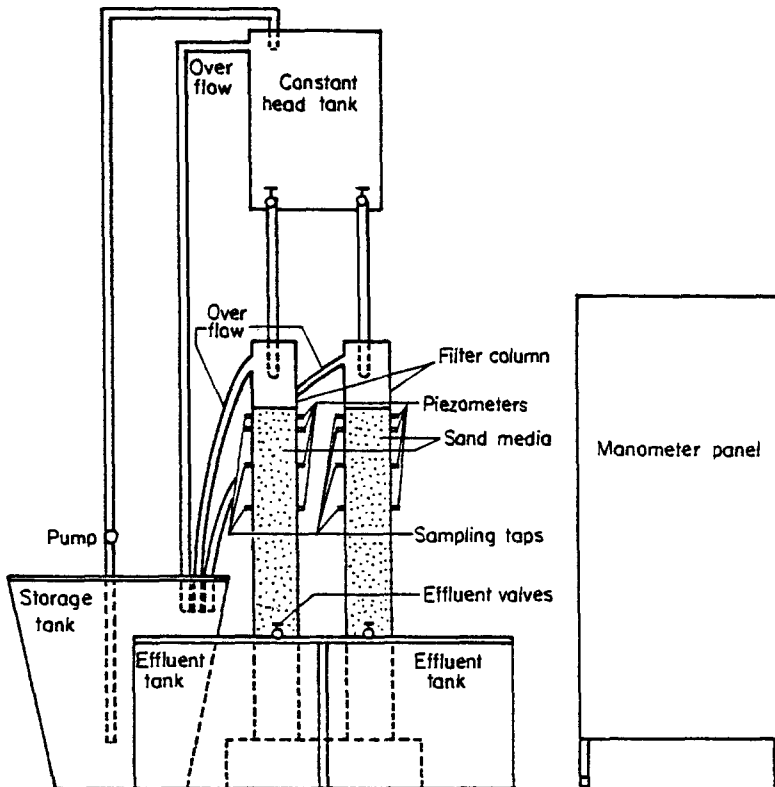


Fig. 1. Experimental set up; scale 1 cm = 10 cm.

Table I shows the physical characteristics of the clean sand packed in each column. The wastewater characteristics are summarized in Table II. For each experimental run, two columns were used, each with a different sand size but of approximately the same infiltration rate. The total volumes of discharge of each unit were measured to determine their respective cumulative discharges.

Sampling for DO measurement was done by using a 60-mL syringe. It was inserted into the sampling tap and the sample was drawn very slowly to eliminate possible destruction of the microbial growth. Fifty mL of the sample was analyzed and proportionate volumes of reagents (0.35 mL each of manganous sulfate, alkali azide

TABLE I
Experimental operations parameters

Run No.	Sand size (mm)	Geometric mean sand size (mm)	Initial infiltration rate (q_0)	Porosity (f)	Media depth (cm)
1	(0.297–0.840)	0.50	3.56	0.397	50.5
	(0.105–0.297)	0.18	3.31	0.382	50.5
2	(1.000–1.168)	1.08	8.43	0.408	50.5
	(0.590–0.840)	0.70	8.43	0.400	50.5
3	(1.000–1.168)	1.08	22.50	0.408	50.5
	(0.500–0.840)	0.70	22.25	0.400	50.5
4	(0.297–0.840)	0.50	11.08	0.397	50.5
	(1.000–1.168)	1.08	11.98	0.408	50.5

TABLE II
Recharging water characteristics

Parameters	Range of concentrations (mg L ⁻¹)
(a) Suspended solids (SS)	40–102
(b) Dissolved oxygen (DO)	6.7–7.2
(c) 3-day biological oxygen demand (BOD ₃)	14.2–21.0
(d) Total organic carbon (TOC)	12–14.5
(e) Total chemical oxygen demand (COD _t)	115–165
(f) Filtered chemical oxygen demand (COD _f)	58–78

iodide and concentrated H₂SO₄) were added for the azide modification of DO analysis (American Waterworks Association, American Public Health Association and Water Pollution Control Federation, 1981).

Biological oxygen demand (BOD) was measured in terms of BOD₃ (i.e., 3 days incubation at 30 °C). Excellent correlation had been found between BOD₃ at 30 °C and BOD₅ at 20 °C. Headloss was measured directly from piezometer readings. Chemical oxygen demand (COD) and total organic carbon (TOC) were analyzed according to standard procedures (American Waterworks Association, American Public Health Association, and Water Pollution Control Federation, 1981).

4. Discussion of Results

4.1. VARIATION OF INFILTRATION RATE

It can be seen from Figures 2(a), 3(a), 4(a), 5(a), 6(a), and 7(a) that the temporal variation of the infiltration rate has three stages in agreement with the results obtained

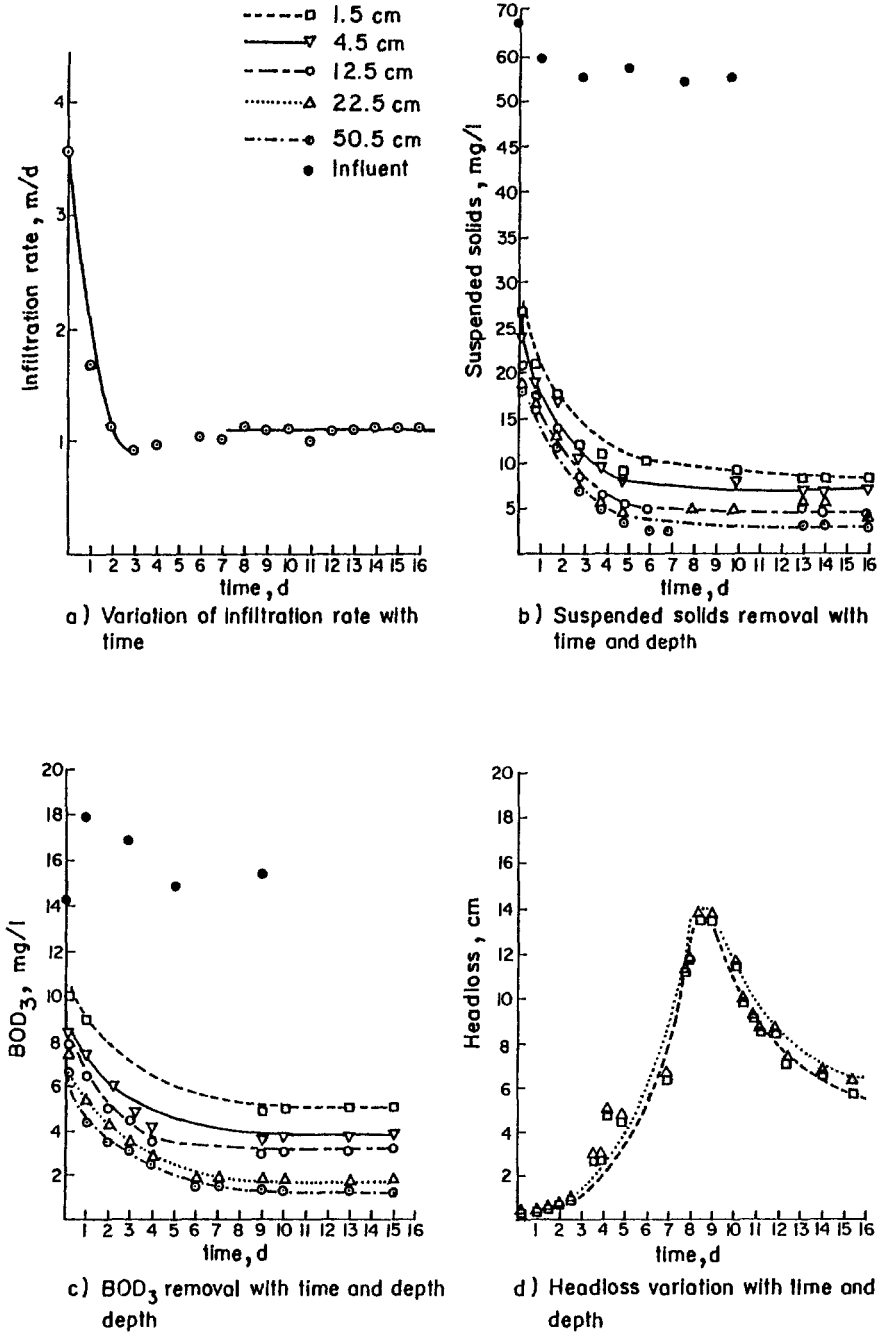
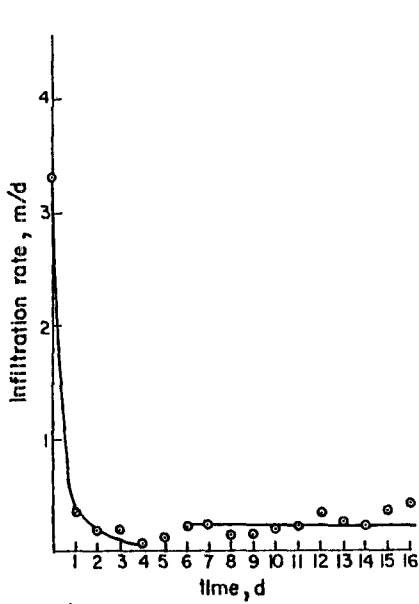
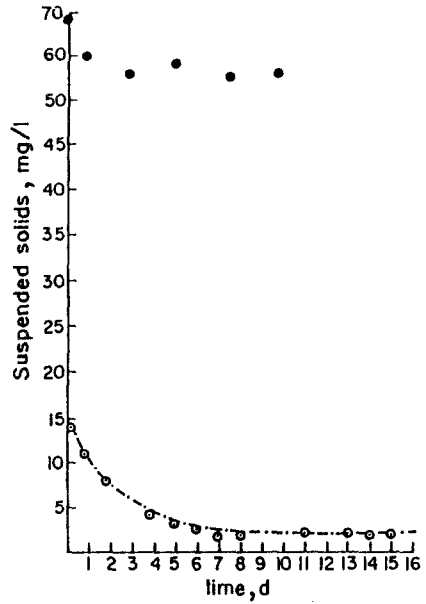


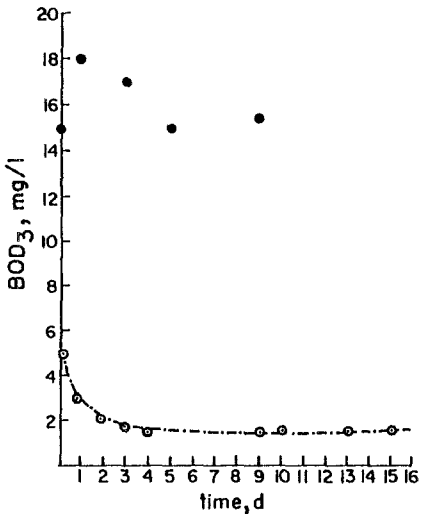
Fig. 2. Variation of infiltration rate, suspended solids and BOD₃ removal and headloss with time and depth ($d_g = 0.50$ mm; $L = 50.5$ cm; $q_0 = 3.56$ m day⁻¹).



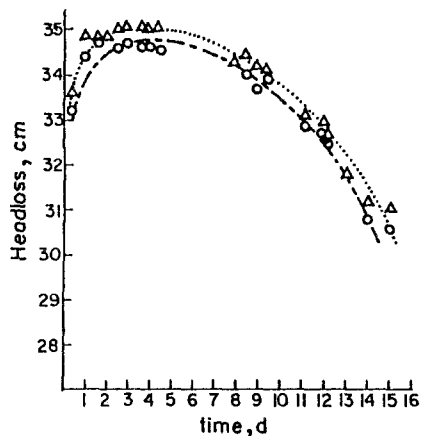
a) Variation of Infiltration rate with time



b) Variation of suspended solids concentration with time and depth



c) BOD₃ removal with time and depth



d) Headloss variation with time and depth

Fig. 3. Variation of infiltration rate, suspended solids and BOD₃ removal and headloss with time and depth ($d_g = 0.18$ mm; $L = 50.5$ cm; $q_0 = 3.31$ m day⁻¹).

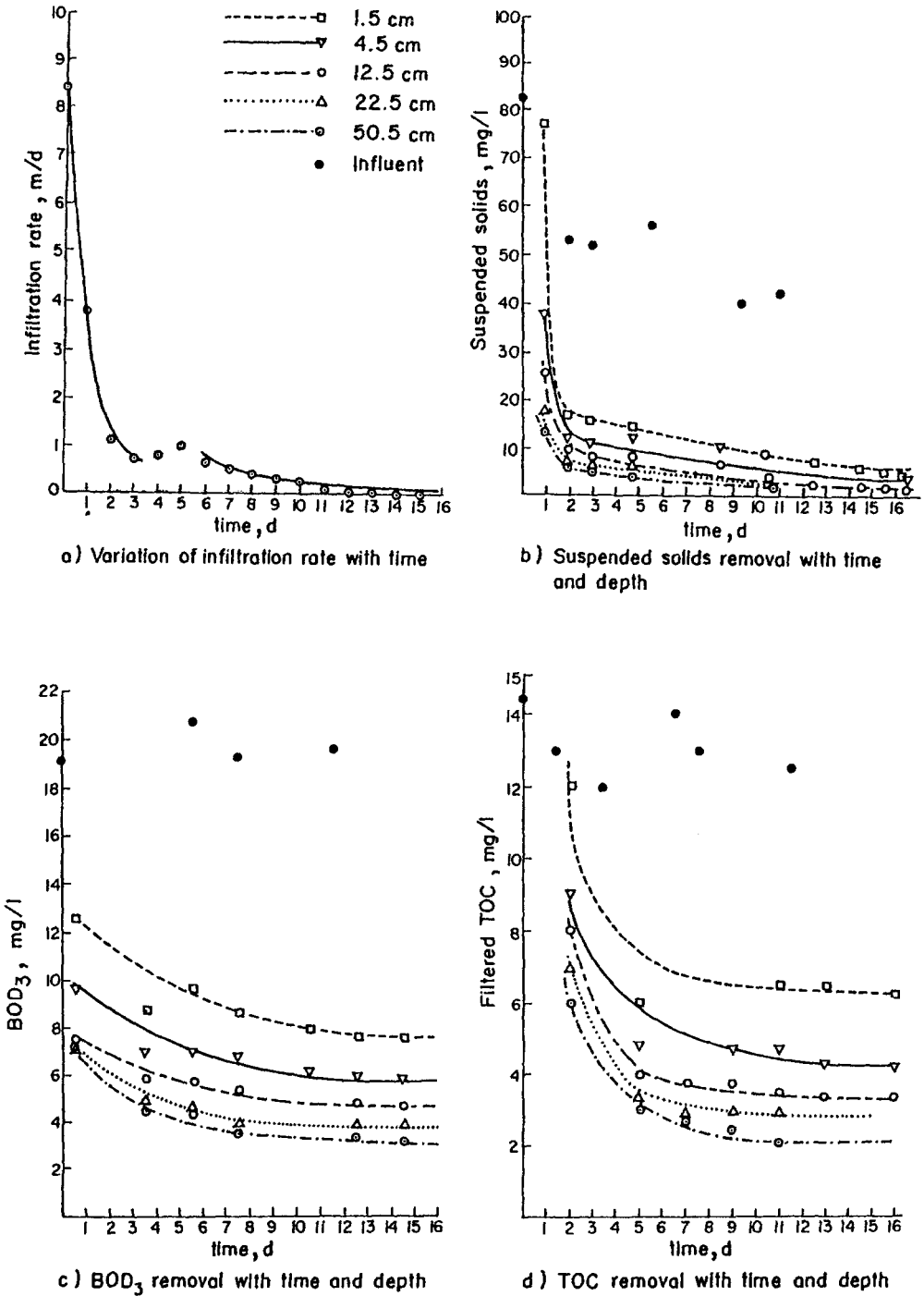


Fig. 4. Variation of infiltration rate, suspended solids, BOD₃ and TOC removal with time and depth ($d_g = 0.70$ mm; $L = 50.5$ cm; $q_0 = 8.43$ m day⁻¹).

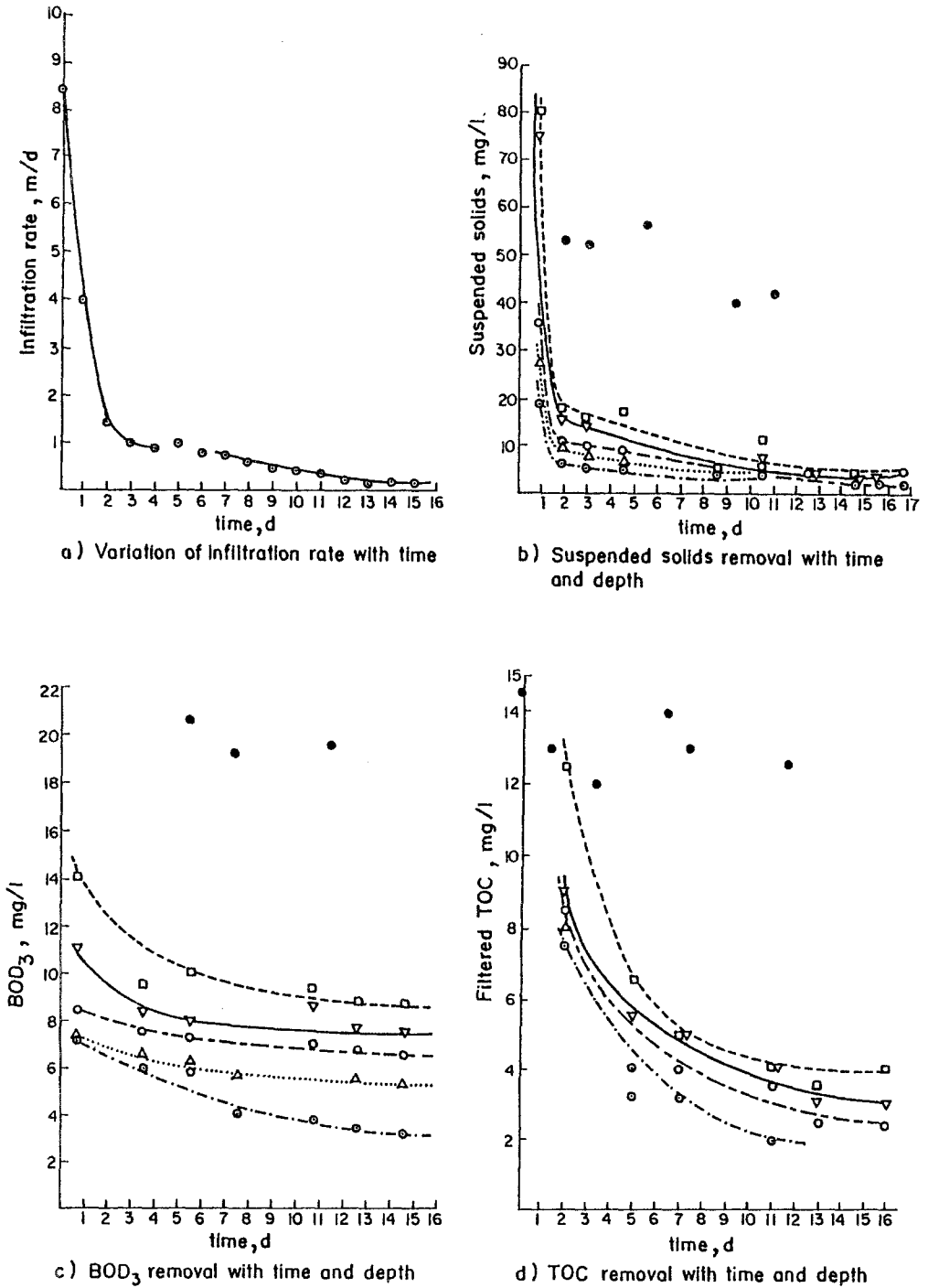


Fig. 5. Variation of infiltration rate, suspended solids, BOD₃ and TOC removal with time and depth ($d_g = 1.08$ mm; $L = 50.5$ cm; $q_0 = 8.43$ m day⁻¹).

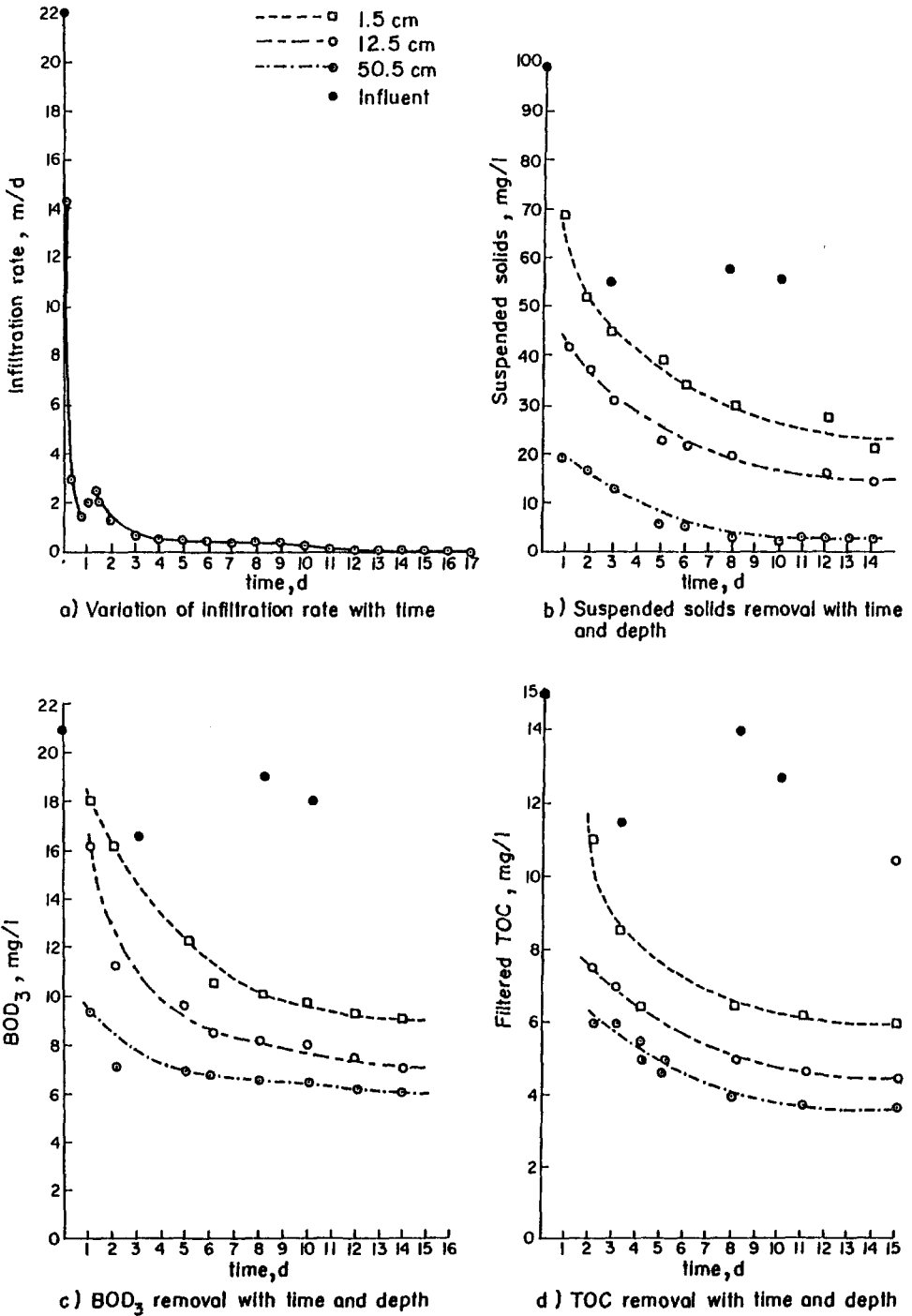
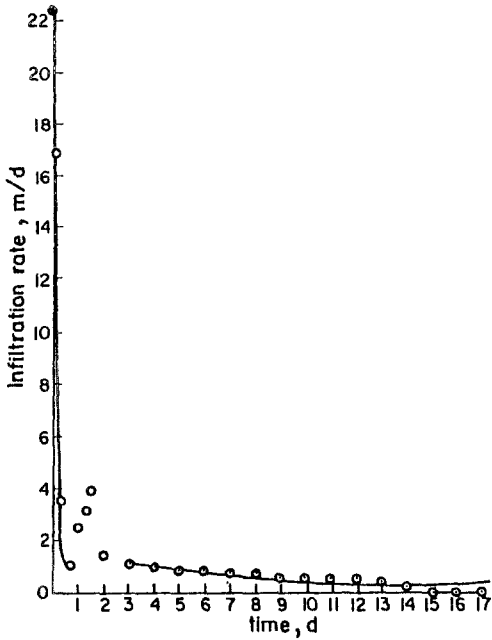
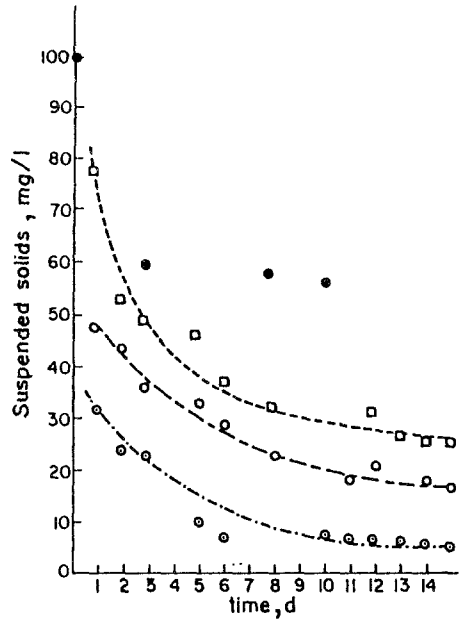


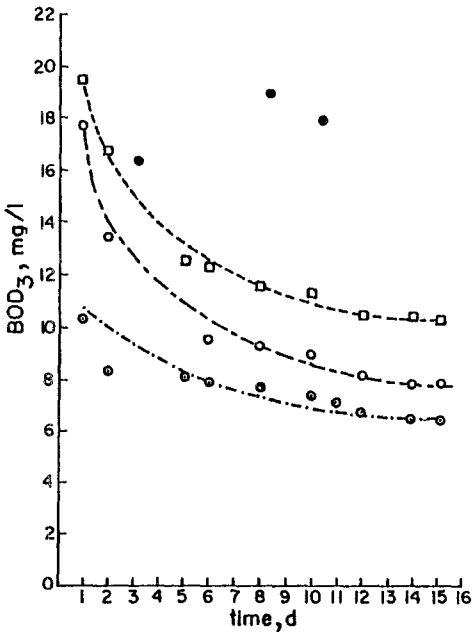
Fig. 6. Variation of infiltration rate, suspended solids, BOD₃ and TOC removal with time and depth ($d_g = 0.70$ mm; $L = 50.5$ cm; $q_0 = 22.25$ m day⁻¹).



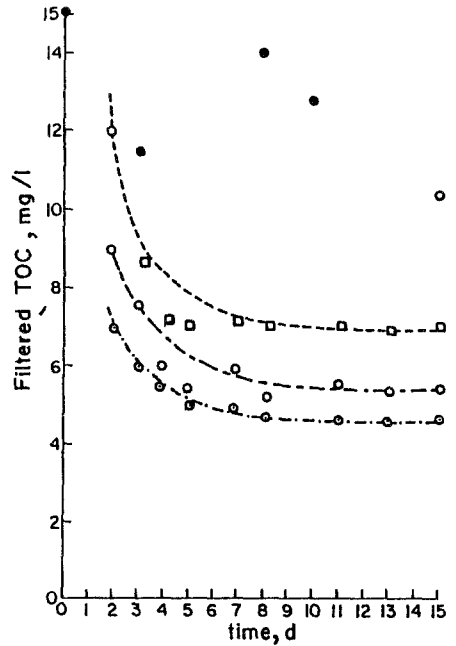
a) Variation of infiltration rate with time



b) Suspended solids removal with time and depth



c) BOD₃ removal with time and depth



d) TOC removal with time and depth

Fig. 7. Variation of infiltration rate, suspended solids, BOD₃ and TOC removal with time and depth ($d_g = 1.08$ mm; $L = 50.5$ cm; $q_0 = 22.50$ m day⁻¹).

by Okubo and Matsumoto (1983). The first stage is characterized by a rapid decrease in the infiltration rate due to the rapid decrease in the porosity by suspended solids retention and microbial growth in the sand, especially at the top portion of the bed. In this study, the first stage occurred during the first four days at low infiltration rates (3.31 and 3.56 m day⁻¹). This period became shorter as the initial infiltration rate was increased. For example, this period was only for a day when the infiltration rate was increased to 22.25 m day⁻¹.

A slower decrease and a slight increase in the infiltration rate characterized the second stage. This may be due to the combined effects of inhibited microbial growth resulting from limited DO supply and continued suspended solids deposition. This period occurred from the fifth day to the sixth day at an infiltration rate of 3.56 m day⁻¹. At the high infiltration rate of 22.25 m day⁻¹, it occurred during the second to the fourth day.

The final stage is characterized by a gradual decrease in the infiltration rate until the column gets clogged. In addition to the accumulated suspended solids, the microbial growth could have been a factor in the clogging (Allison, 1947; Ripley and Saleem, 1973).

The relationship of the cumulative discharge with the inundation period can be represented by Equation (1), which was originally proposed by Okubo and Matsumoto (1983).

$$Q = \frac{K_1 q_0 t}{K_2 + t}, \quad (1)$$

in which,

K_1 = limit of Q/q_0 for an increasing inundation period of t , day,

K_2 = inundation period at which Q/q_0 is half the maximum, day,

Q = cumulative discharge, m³/m²,

q_0 = initial infiltration rate, m day⁻¹, and

t = inundation period.

The values of K_1 and K_2 can be obtained directly from their definitions. K_1 is the ratio of the cumulative discharge and the initial infiltration rate at an inundation period of

TABLE III
 K_1 and K_2 values of the different experimental runs

Run No.	Geometric mean sand size (mm)	Infiltration rate (m day ⁻¹)	K_1 (day)	K_2 (day)
1	0.50	3.56	5.00	8.10
	0.18	3.31	1.20	10.30
2	1.08	8.43	1.43	2.50
	0.70	8.43	1.24	2.30
3	1.00	22.50	0.74	3.00
	0.74	22.25	0.46	1.50

t while K_2 is the inundation period at which the above ratio is half the maximum. The values of K_1 and K_2 obtained in this manner for different conditions are summarized in Table III. It can be seen that the K_1 and K_2 values are inversely proportional to the infiltration rate and, in general, directly proportional to the sand size. The simulated cumulative discharge profiles calculated with the K_1 and K_2 values using Equation (1)

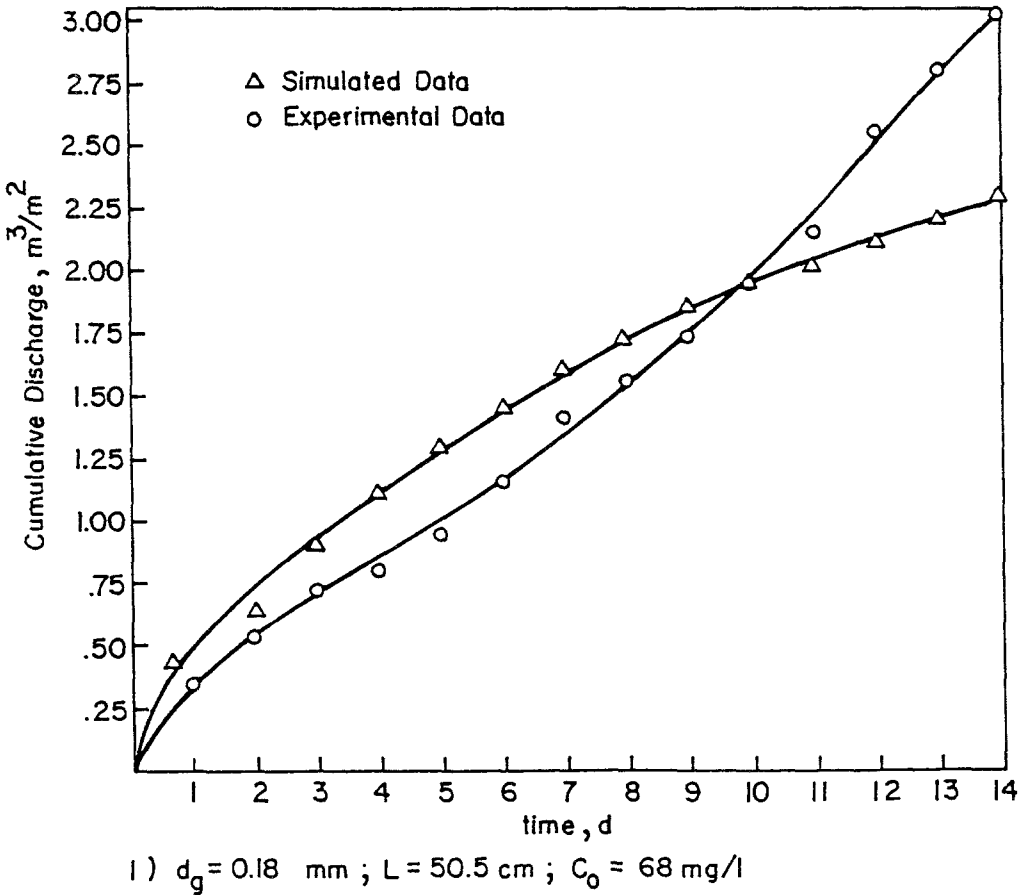
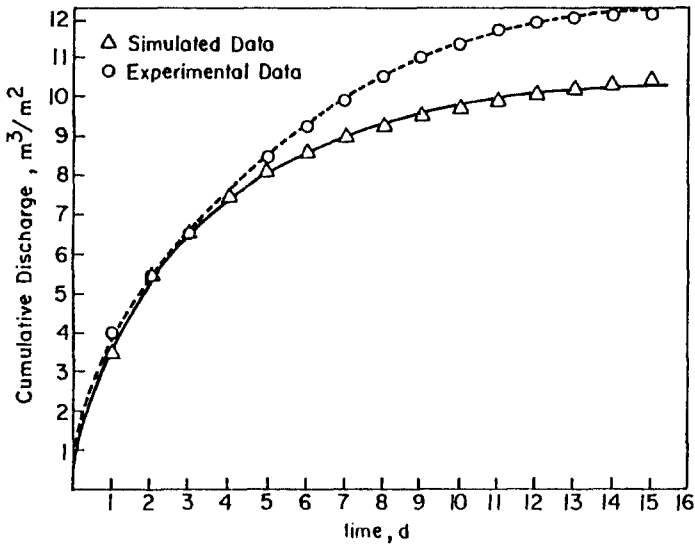


Fig. 8. Experimental and theoretical cumulative discharge profiles at an initial discharge rate of 3.31 m day^{-1} .

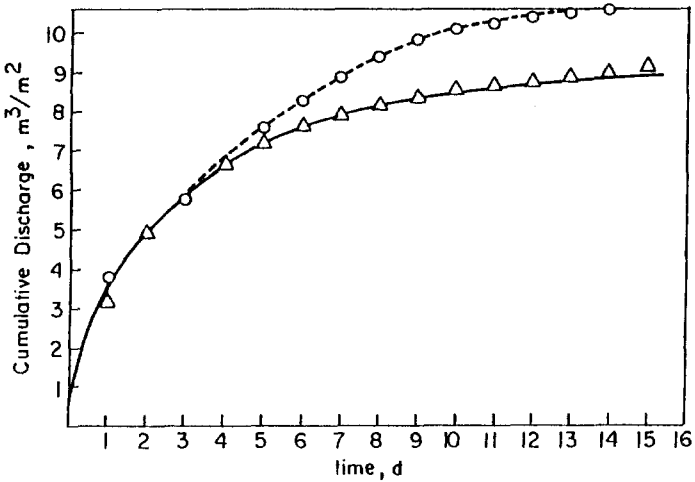
are presented in Figures 8, 9, and 10 along with the experimental profiles. This indicates that an empirical relationship established between K_1 , K_2 , and q_0 from laboratory-scale experiments can successfully be used to predict the biological clogging at different rates.

4.2. BIOLOGICAL CLOGGING

The clogging in this particular study is mainly due to biological solids removal within the sand pores. Biological solids removal was studied in terms of suspended solids



1) $d_g = 1.08 \text{ mm}$; $L = 50.5 \text{ cm}$; $C_0 = 84 \text{ mg/l}$



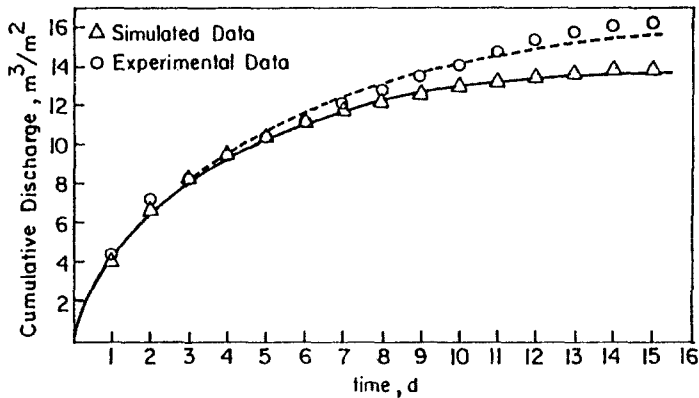
2) $d_g = 0.70 \text{ mm}$; $L = 50.5$; $C_0 = 84 \text{ mg/l}$

Fig. 9. Experimental and theoretical cumulative discharge profiles at an initial discharge rate of 8.43 m day^{-1} .

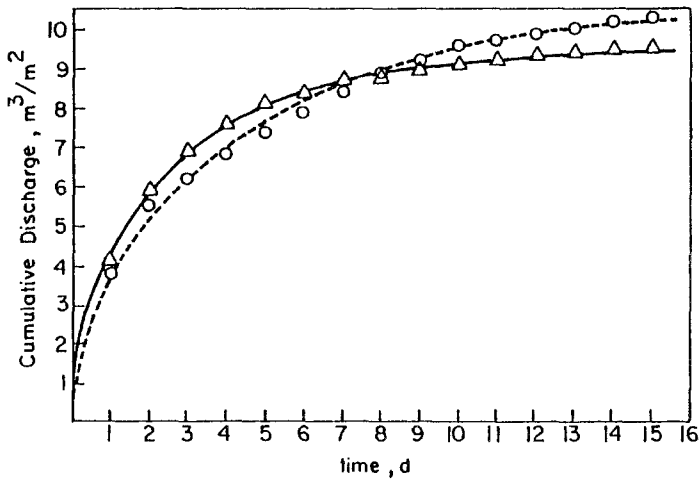
removal, headloss development, and temporal variation of BOD_3 , COD, and DO for different operating conditions of recharge.

4.2.1. *Suspended Solids Removal*

Figures 2b, 3b, 4b, 5b, 6b, and 7b show that the suspended solids removal efficiency increases rapidly at the initial stages and remains almost constant afterwards. This



1) $d_g = 1.08 \text{ mm}$; $L = 50.5 \text{ cm}$; $C_0 = 100 \text{ mg/l}$



2) $d_g = 0.70 \text{ mm}$; $L = 50.5$; $C_0 = 100 \text{ mg/l}$

Fig. 10. Experimental and theoretical cumulative discharge profiles at initial discharge rates of 22.50 m day^{-1} and 22.25 m day^{-1} , respectively.

improvement of the removal efficiency at the initial stages was probably due to the accumulated suspended solids and the microbial growth within the filter bed. The latter predominates at the later stage of filtration. The finer the medium and the lower the infiltration rate, the better is the removal efficiency, as one would generally expect. Surface mat formation of suspended solids was more significant at the infiltration rate of 8.43 m day^{-1} (Figures 4b and 5b). The major suspended solids removal in this case was confined to the top 12.5 cm. At the highest initial infiltration rate, the suspended solids were distributed within the entire bed (Figures 6b and 7b). Similarly, the large filter media led to better distribution of the suspended solids in the bed.

4.2.2. Headloss

The previous works on deep bed filtration indicate that headloss development with time is linear at the initial stages and exponential at the later stages. But in this study, the headloss profiles (Figures 2d, 3d, 11a, and 11b) show a decreasing trend. For example, in the last experimental run the decreasing trend was observed between the ninth and twentieth day (Figures 11a and 11b). The decomposition of retained particles may have

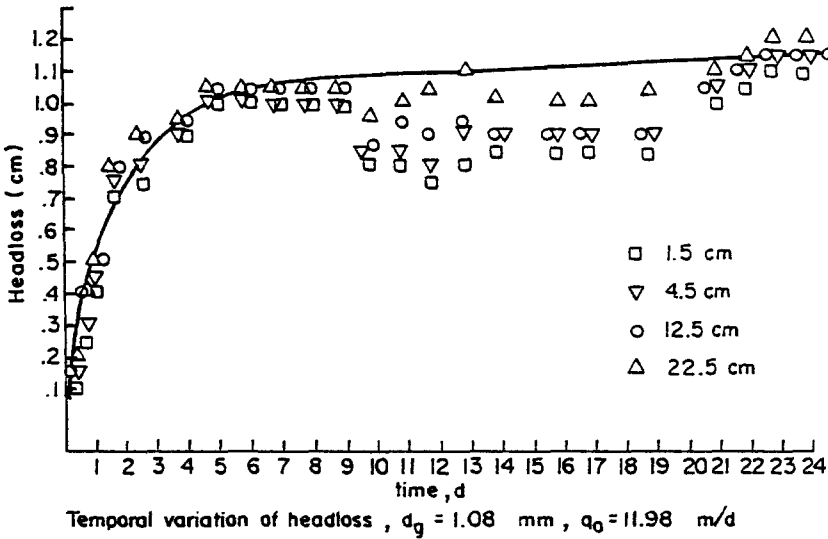


Fig. 11a. Temporal variation of headloss.

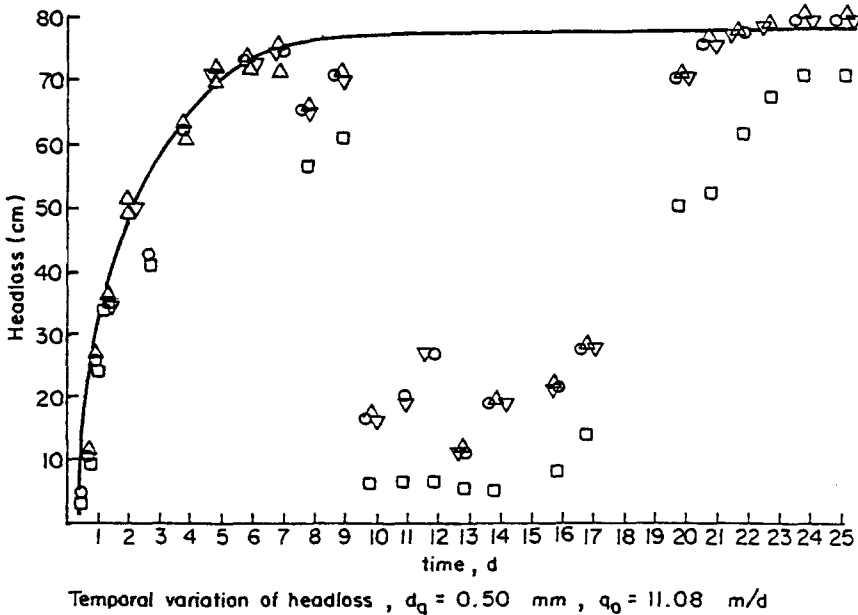


Fig. 11b. Temporal variation of headloss.

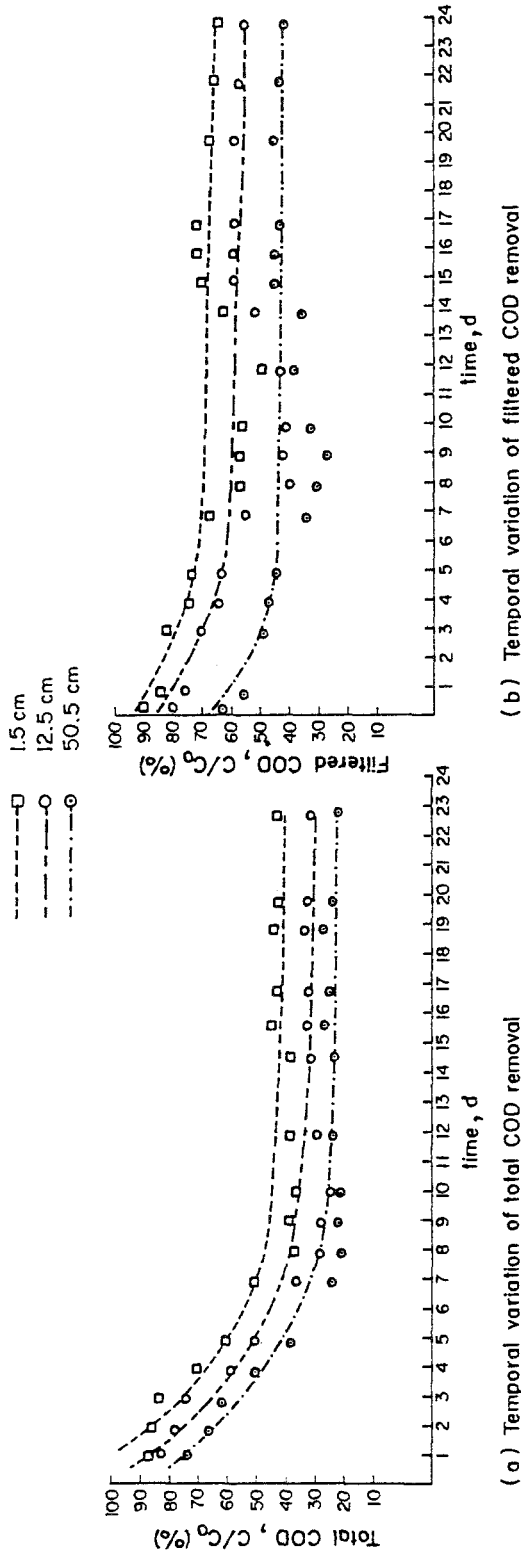
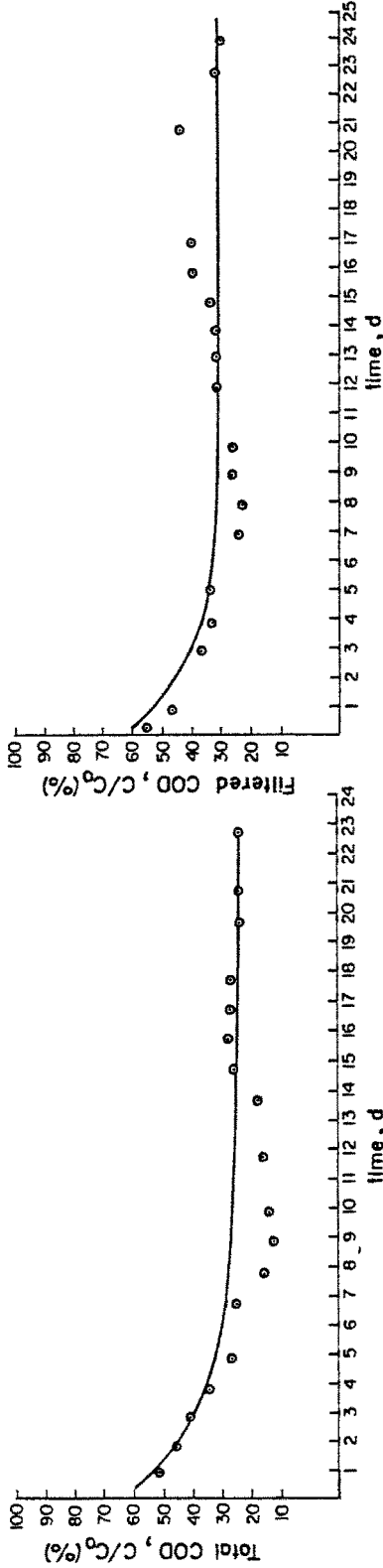


Fig. 12. Temporal variation of infiltration rate, suspended solids, total COD removal ($d_g = 1.08$ mm; $L = 50.5$ cm; $q_0 = 11.98$ m day⁻¹).



(a) Temporal variation of total COD removal

(b) Temporal variation of filtered COD removal

Fig. 13. Temporal variation of infiltration rate, suspended solids, total COD and filtered COD removal ($d_g = 0.50$ mm; $L = 50.5$ cm; $q_0 = 11.08$ m day⁻¹).

caused this decrease in headloss. Okubo and Matsumoto (1979 and 1983) also observed the same phenomenon at the top portion of the filter column. It is also possible that the decomposition of the biological matter into soluble compounds may have caused this headloss behavior. A decrease in COD removal efficiency observed during this stage (Figures 12 and 13) may be an indication of the decomposition of biological matter.

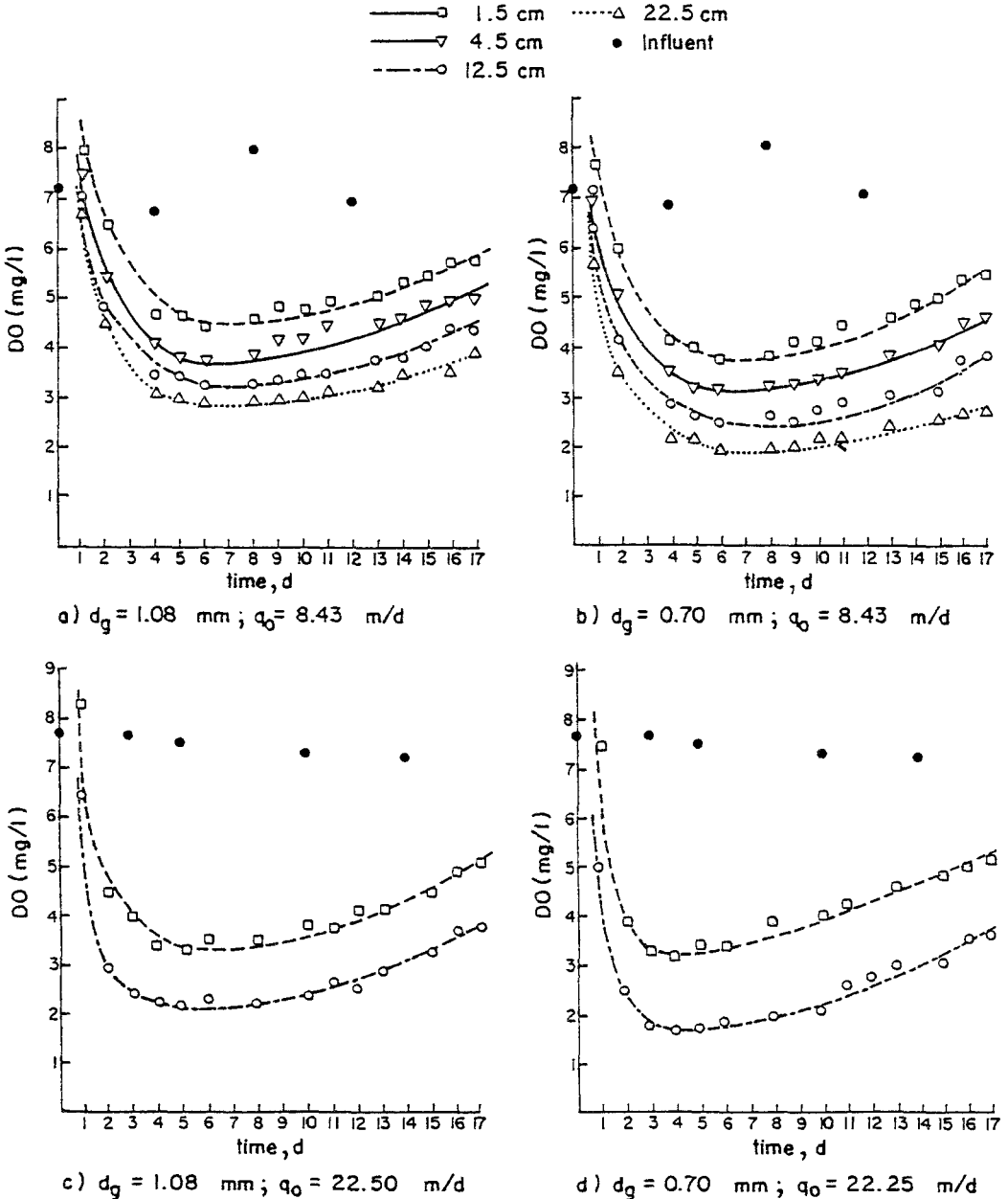
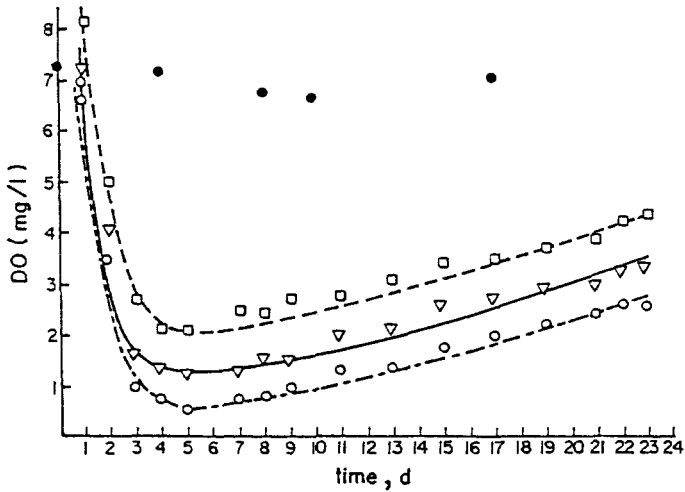


Fig. 14. Temporal variation of DO with depth.



e) Temporal variation of DO ; $d_g = 1.08$ mm ; $q_0 = 11.98$ m/d

The headloss profiles drawn for various depths indicate that the major headloss development is confined to the top 1.5 cm depth and that there is no significant headloss in the succeeding layers, thus supporting the phenomenon of surface mat formation.

In addition to this, the prevalence of low DO conditions was observed prior to this stage (Figure 14). This low DO condition would have inhibited the prevailing microbial growth. Thus, detachment could have occurred.

4.2.3. BOD_3 and COD-removal

The BOD_3 removal efficiency increased with time at the early stages and then remained constant (Figures 2(c), 3(c), 4(c), 5(c), 6(c), and 7(c)). The major mechanism involved was the same as that responsible for suspended solids removal-surface straining. Smaller sand sizes and lower infiltration rates resulted in better BOD_3 removal as in the case of suspended solids removal.

With respect to renovation, the maximum BOD_3 removal efficiency was 94.6% for the 0.18 mm diameter sand and an initial infiltration rate of 3.31 m day^{-1} . For the 0.50 mm sand and an initial infiltration rate of 3.56 m day^{-1} removal efficiency was 93%. The removal efficiency was 84% with 1.08 mm diameter sand and an infiltration rate of 8.43 m day^{-1} . At the high infiltration rate of 22.50 m day^{-1} , BOD_3 removal efficiency was only 64% for the 1.08 mm diameter sand and 67% for the 0.70 mm diameter sand.

The steady-state condition can be best analyzed using the values of the reaction rate coefficient, k , at different filter depths by the following equation:

$$\ln(c/c_0) = -kT \quad (2)$$

in which,

$$\begin{aligned}
 c &= \text{effluent BOD}_3 \text{ concentration, mg L}^{-1}, \\
 c_0 &= \text{influent BOD}_3 \text{ concentration, mg L}^{-1}, \\
 k &= \text{reaction rate constant, day}^{-1}, \text{ and} \\
 T &= \text{detention time (day)}.
 \end{aligned}$$

The values of k obtained at different conditions are summarized in Table IV. It can be seen that the reaction rate coefficient, k , decreases with depth. Significant differences in k values were observed between 0 to 1.5 cm and 1.5 to 4.5 cm, whereas the differences narrowed for the 1.5 to 4.5 cm and 4.5 to 12.5 cm depths. The higher k -values at the top 1.5 cm indicate high reaction rates at the top 1.5 cm. At high infiltration rates, the variation of k values along the depth is not as high as when the infiltration rate is low. In other words, at high infiltration rates, the biological reaction is distributed along the depth, whereas it is confined to the top few centimeters at low infiltration rates. Similarly, the use of a large filter medium resulted in better distribution of the biological reaction in the bed.

TABLE IV

Values of the steady-state reaction rate coefficient at different depths, infiltration rates, and sand sizes

d_g (mm)	V (m day ⁻¹)	k , average (day ⁻¹)			Elapsed time when steady-state occurred (day)
		1.5 cm	4.5 cm	12.5 cm	
0.50	3.56	81.34	3.17	0.87	7
0.70	8.43	21.35	2.16	0.75	7
1.08	8.43	18.83	1.41	0.46	7
0.70	22.25	11.58	–	0.74	5
1.08	22.50	18.64	–	1.25	5

Total COD removal efficiency also increased with filter medium depth, and, to a certain limit, with time. Figures 12 and 13 show that both the total and filtered COD removal efficiency increased up to the tenth and ninth day, respectively, and gradually decreased afterwards. It is possible that effluent COD concentrations began to increase as a result of the decomposition of suspended solids and microbial growth. It can be noticed that this period coincided with the headloss phenomenon explained previously.

The maximum total COD renovation, as expected, was higher for the column with smaller effective sand size: 86% for the column with a sand of 0.50 mm in size and an initial infiltration rate of 11.08 m day⁻¹ and 75% for the column with a sand of 1.08 mm in size and an initial infiltration rate of 11.98 m day⁻¹.

5. Conclusion

From the results of the experiments the following conclusions can be made:

- The temporal variation of the infiltration rate was found to occur in three distinct stages.

- The rate of decrease in the infiltration rate was faster when higher initial infiltration rates were applied through the sand columns.
- The values of K_1 and K_2 obtained from their definitions have been found to successfully predict the biological clogging at different recharge rates.
- An improvement in suspended solids and BOD_3 removal was observed at the early stages of recharge, followed by an almost constant removal. The improvement of the removal rate was fast at higher infiltration rates but the steady state was obtained within a short period.
- A decrease in headloss with time was observed after an initial increase. This may be attributed to the following: decomposition of retained biological solids and microbial growth and/or decomposition of biological matter into soluble compounds.
- The major removal is confined to the top few centimeters of the bed. The reaction rate constant calculated at the top 1.5 cm of the bed was 10 to 20 times higher compared to the next layer (at 1.5 to 4.5 cm).

References

- Allison, L. E.: 1947, *Soil Science* **63**, 439.
- American Waterworks Association, American Public Health Association, and Water Pollution Control Federation: 1981, *Standard Methods for the Examination of Water and Wastewater*, 4th edition, American Public Health Association, Washington D.C.
- Amramy, A.: 1965, *J. Air Water Pollut.* **9**, 605.
- Avnimelech, Y. and Nevo, Z.: 1964, *Soil Science* **98**, 222.
- Besty, R. J.: 1980, Burdekin Artificial Groundwater Recharge Study: Biological Problems in Artificial Recharge of Groundwater, AWRC Groundwater Recharge Conference, Townsville, Australia.
- De Vries, J.: 1972, *J. Water Pollut. Control Federation* **44**, 565.
- Fetter, C. W. and Holzmacher, R. G.: 1974, *J. Water Pollut. Control Federation* **46**, 260.
- Harpaz, Y.: 1970, Practical Experiences of Well Recharge, Proceedings of Artificial Groundwater Recharge Conference, Water Research Association, England.
- Huisman, L. and Olsthoorn, T. N.: 1983, *Artificial Groundwater Recharge*, John Wiley and Sons, New York.
- Lance, J. C. and Whistler, F. D.: 1973, Nitrogen Removal During Land Filtration of Sewage Water, Canadian Society of Soil Science, Proceedings of the International Conference on Land for Waste Management, Canada.
- Mitchell, R. and Nevo, Z.: 1964, *Applied Microbiology* **12**, 219.
- Nevo, Z. and Mitchell, R.: 1967, *Water Research* **1**, 231.
- Okubo, T. and Matsumoto, J.: 1979, *Water Resources Research* **15**, 1532.
- Okubo, T. and Matsumoto, J.: 1983, *Water Resources Research* **17**, 813.
- Ripley, D. P. and Saleem, Z. A.: 1973, *Water Resources Research* **9**, 1047.
- Thiyagaram, M.: 1982, 'Three-Dimensional Filtration Models and their Application to Groundwater Recharge Problems', Master's Thesis, Asian Institute of Technology, Bangkok, Thailand.
- Todd, D. K.: 1959, *Groundwater Hydrology*, 2nd edition, John Wiley and Sons, New York.
- Vecchioli, J. and Ku, H.: 1971, Preliminary Results of Injecting Highly Treated Sewage-Plant Effluent into a Deep Sand Aquifer at Bay Park, New York, U.S. Geological Survey Report.
- Vigneswaran, S., Jeyaseelan, S., and Das Gupta, S.: 1985, *Water, Air, and Soil Pollut.* **25**, 1.
- Vigneswaran, S. and Thiyagaram, M.: 1984, *Water, Air, and Soil Pollut.* **22**, 417.
- Winquist, G. and Marelius, K.: 1970, The Design of Artificial Recharge Schemes, Proc. Artificial Groundwater Recharge Conference, Water Research Association, England.
- Wood, W. W. and Bassett, R. L.: 1975, *Water Resources Research* **11**, 553.